Excitation of the $a\,^3\Pi$ state of CO by electron impact

M. M. Ristić

University of Belgrade, Faculty of Physical Chemistry, Studentski trg 12-16, P.O. Box 137, 11000 Belgrade, Serbia

G. B. Poparić[*] and D. S. Belić

University of Belgrade, Faculty of Physics, Studentski trg 12-16, P.O. Box 368, 11000 Belgrade, Serbia

Electron impact excitation of the $a\,^3\Pi$ valence state of the carbon-monoxide molecule has been studied in the energy region from threshold to 10 eV. Excitation functions for spin forbidden transitions from the $v = 0$ level of the ground $X\,^1\Sigma^+$ state of CO to the $v' = 0, 1, 2, 3, 4$, and 5 levels of the $a\,^3\Pi$ state are measured. A crossed beam double trochoidal electron spectrometer is used. Forward and backward scattered electrons from the $v' = 0$ excitation channel are separated by electron beam modulation and a time-of-flight detection technique. The present results are normalized to the ground state $^2\Pi$ resonance vibrational excitation cross sections and absolute values of the differential cross sections at the border angles of $0°$ and $180°$ are determined. In this way the differential cross section measurements are completed in the full angular range from $0°$ to $180°$. The present results are compared to the existing literature data.

I. INTRODUCTION

Electron collision processes with carbon monoxide are important in plasma and discharge technology, chemical detectors, and in laser devices [1,2]. Since CO is a constituent of Earth's as well as Mars and Venus atmospheres, studies of electron impact excitation of CO are also of interest for planetary astrophysics [3]. Electron impact excitation is also recognized as an important mechanism for producing CO in the $a\,^3\Pi$ state, which has been detected via spin-forbidden Cameron bands in UV spectra of Mars and of other galactic objects beyond the Solar System [4].

Resonant phenomena in vibrational and electronic excitation of diatomic molecules have been reviewed by Schulz [5], by Trajmar *et al.* [6], and more recently by Brunger and Buckman [7]. First measurements of differential cross sections (DCSs) for electronic excitation of the $a\,^3\Pi$ electronic state of the carbon-monoxide molecule, with a threshold energy of 6.01 eV, were carried out by Trajmar *et al.* [8], but only for the single electron energy of 20 eV and in the angular range from $10°$ to $90°$. Middleton *et al.* [9] measured DCSs and integral cross sections (ICSs) in the same angular range in the energy region from 20 to 50 eV. Later measurements of Trajmar's group [10,11] were carried out in the near-threshold energy region and absolute DCS and ICS for electron energies from 6 to 15 eV, and in the angular range from $5°$ to $135°$ have been reported.

Zobel *et al.* [12] performed a very detailed experimental study of the near-threshold $a\,^3\Pi$ state electron impact excitation. Both excitation functions and angular dependencies have been reported in the energy range from threshold to 9.7 eV and in the angular range from $20°$ to $140°$. The measurements were performed for excitation of the $v' = 0, 1, 2, 3, 4$, and 5 vibrational levels of the $a\,^3\Pi$ state. The DCS values were put on the absolute scale by means of the relative flow technique [13]. Corresponding ICSs values have also been reported. The

shapes of these ICSs versus energy coincide to the *R*-matrix calculations performed by Morgan and Tennyson [14] in the energy region from 6 to 18 eV. This agreement has confirmed the prediction that at least three resonances are involved in the resonant excitation of the $a\,^3\Pi$ state: $^2\Pi$, $^2\Delta$, and $^2\Sigma$.

Theoretical investigations of the resonant $a\,^3\Pi$ state excitation have also been performed by Mu-Tao and McKoy [15] in the 20–50 eV energy range, by Sun *et al.* [16] employing a Schwinger multichannel (SMC) variational method from threshold to 30 eV, and by Mu-Tao *et al.* [17] with distorted-wave (DW) calculations in the 20–100 eV range. In all of these calculations both DCSs and ICSs have been reported for total, vibrationally nonresolved excitation.

The ICSs have also been measured by Ajello [18], Brongersma *et al.* [19], Land [20], Newman *et al.* [21], and Furlong and Newell [22], while theoretical predictions of ICSs have been reported by Chung and Lin [23].

In the present experiment excitation functions for the $v' = 0, 1, 2, 3, 4$, and 5 levels of the $a\,^3\Pi$ state of CO are measured. Forward and backward scattered electrons from the $v' = 0$ excitation channel are separated by an electron beam modulation and time-of-flight detection technique. Present results are normalized to the ground state $^2\Pi$ resonance vibrational excitation cross sections of CO and absolute values of the differential cross sections at the border angles of $0°$ and $180°$ are determined.

II. EXPERIMENTAL SETUP

The present measurements are performed by using a crossed beam double trochoidal (TEM) electron spectrometer. It has been described in detail elsewhere [24–26], and so only a brief outlook will be given here. A monoenergetic electron beam is crossed at right angles with the CO gas beam. After the collision, electrons scattered in the forward (and backward) direction are analyzed by use of a double TEM device [24–28] and detected by a channel electron multiplier.

Due to the presence of a longitudinal magnetic field, in the originally designed apparatus the detected signal consists of

---

*Goran_Poparic@ff.bg.ac.rs

the sum of electrons inelastically scattered at 0° and 180° within the same solid angles at the given residual energy [26–28]. Inelastic electrons scattered at 180°, which move backward along the incident electron beam trajectory, are reflected at the potential barrier in front of the collision chamber, reach again the collision region, and from there follow the same path as the forward scattered electrons. Thus they travel a longer distance and need a longer time to reach the detector. This fact is used to separate these two groups of electrons by recording their time-of-flight spectra.

For this kind of measurement the incident electron beam needs to be pulsed in an appropriate way. In the present experiment electron beam chopping is enabled by a 1.18 MHz square-shaped asymmetric pulse generator. Square pulses of 50 ns, 2 V high, are separated by 800 ns. This signal is superimposed on the voltage of one electrode after the TEM. The potential of this electrode keeps the electron beam on during 50 ns of the pulse time and off for the rest of the time. The rising time of the pulses can be used as a trigger of the time-to-amplitude converter (TAC). In fact, this signal is used as a stop trigger of the TAC. For the start of the TAC the signal from the channeltron detector is used. Therefore each recorded event represents the time difference between electron detection and the next pulse coming from the generator. This inverted arrangement has no influence on the results, but can improve the detection efficiency of the experiment.

This procedure has been successfully applied to separate forward and backward scattered electrons from the $E\,^3\Sigma_g^+$ state resonant excitation of the N_2 molecule [25]. Measurements in that case were performed with a low-residual electron energy (67 meV). For faster, more energetic electrons, however, backward scattered electrons need to be decelerated. In that way the time difference of their arrival to the detector can be increased. For this purpose a decelerator device has been introduced in front of the collision region. It consists of two parallel plates, 20 mm long. They are kept at a low negative potential below the interaction region, so that backward scattered electrons travel with low velocity back and forth over this distance and so spend some 80–100 ns in this device before entering again the collision region from the opposite direction. The operation of the decelerator device has been successfully tested and applied in our experiment on the N_2 and CO molecule [26], as well as more recently on H_2 [29].

The signal from the channeltron is processed by a fast charge amplifier, voltage amplifier, and high-voltage filter. Obtained pulses are used for the start signal of the TAC. The output signal from the TAC is loaded to a pulse-height analyzer (PHA) and further to a multichannel analyzer (MCA) system.

III. RESULTS AND DISCUSSION

The present measurements are carried out in three different modes of operation of the experiment. First, an energy loss spectrum or rather a constant residual energy (CRE) spectrum is registered by keeping constant residual energy of the scattered electrons and changing the incident electron energy. In this way the transitions to particular vibrational levels are identified and corresponding energies are determined. At the same time, working under the same experimental conditions (target gas pressure, electron beam current, analyzer and detector tuning conditions, etc.), relative intensities of the cross sections for the ground state $X\,^1\Sigma^+$ vibrational excitation, via the $^2\Pi$ resonance, and the $a\,^3\Pi$ vibrational levels excitation are obtained. These intensities will be used to put the actual measurements on the absolute scale. Second, excitation functions are registered for each considered vibrational transition process by a simultaneous change of the incident and residual electron energy, while keeping their difference equal to the actual excitation energy. Excitation function spectra are recorded for the sum of forward and backward scattered electrons, for excitation of the $\nu' = 0$, 1, 2, 3, 4, and 5 levels. Each of the recorded excitation function spectra has been corrected to the $1/E_r$ transmission dependence [24,27]. And finally, for the selected incident and residual electron energies, forward and backward scattered electrons are separated by means of electron beam modulation and a time-of-flight technique. These measurements are performed for the excitation of the $\nu' = 0$ level only for five selected electron energies of 6.5, 7, 8, 9, and 9.7 eV. Total numbers of forward and backward scattered electrons are proportional to the DCS at 0° and 180° for the specific incident electron energy.

The analysis of the data will begin here with the results of the time-of-flight measurements. A typical time-of-flight spectrum is shown in Fig. 1 for an incident electron energy of 7 eV.

As it can be seen from Fig. 1 the spectrum is composed of two distinct peaks on the time scale. The first, smaller and narrower one located at 500 ns belongs to the electrons scattered at 0° directly to the analyzer and detector. The second, higher peak around 600 ns corresponds to the electrons scattered at 180°. The two peaks are separated for about 100 ns with a slight overlap in the middle. The spectrum is fitted with two arbitrary Gaussian functions and in that way the two contributions of the electrons are separated with a correlation coefficient $R = 0.98$ in this particular case. These two contributions are presented in Fig. 1 by the solid lines. The ratio of differential cross sections at 0° and at 180° is
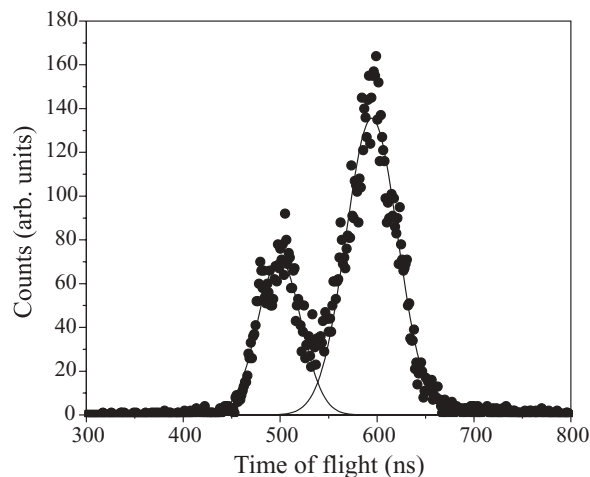
FIG. 1. Time-of-flight spectrum of electrons scattered at 0° and 180° from the $\nu' = 0$ level excitation of the $a\,^3\Pi$ state of CO, at an incident energy of 7 eV.

TABLE I. DCS values (in 10^{-18} cm^2 sr^{-1}) for excitation of the $v' = 0$ level of the $a\,^3\Pi$ state of CO at 0° and 180° and ICS values (in 10^{-18} cm^2) at selected electron energies.

E (eV)	DCS 0°/DCS 180°	DCS 0°	DCS 180°	ICS
6.5	0.65	1.77	2.71	16.62
7.0	0.44	1.32	2.99	21.36
8.0	0.21	0.63	3.07	30.10
9.0	0.22	0.58	2.71	29.05
9.7	0.46	1.01	2.22	23.61

proportional to the ratio of the areas under these two peaks. In this specific case the forward to backward ratio is found to be equal to 1:2.26 (or 0.44).

The results obtained for the ratio of the differential cross sections at 0° and at 180° for all five considered incident electron energies (6.5, 7, 8, 9, and 9.7 eV) are summarized in Table I. They are found to be 0.65, 0.44, 0.21, 0.22, and 0.46, respectively. Estimated error bars are found to be of the order of $\pm 5\%$ (except for 9.7 eV where it is $\pm 10\%$). All listed values are significantly lower than 1, indicating that the DCS value at 180° dominates over the one at 0°. These results are in a very good qualitative agreement with the data of Zobel *et al.* [12].

The absolute value of the sum of the DCS at 0° and 180° for the $v' = 0$ level excitation of the $a\,^3\Pi$ state is normalized to the DCS value of the $v' = 2$ level of the ground state excitation which is largely populated via the $^2\Pi$ resonance. This is performed by employing a measured constant residual energy spectrum recorded for $E_r = 1.46$ eV. The value of 3.48×10^{-17} cm^2 sr^{-1} at the maximum of the $v' = 2$ vibrational level reported by Poparic *et al.* [30] is used. In this way the excitation function measured for the $v' = 0$ level is normalized in a whole electron energy range. By using the forward to backward DCS ratios listed in Table I the absolute DCS values at 0° and at 180° are determined for the considered electron energies. These values are also presented in Table I. In order to calculate DCSs in a whole energy region, the ratios of the DCS at 0° and 180° are extrapolated to all energies by a polynomial fit. This polynomial is used to deduce the absolute DCS values at 0° and at 180° from the normalized excitation function of the sum of forward and backward scattered electrons for all energies. The results from this process are shown in Figs. 2 and 3.

Measured excitation functions for the sum of forward and backward scattered electrons for the $v' = 1$–5 levels are normalized relative to the $v' = 0$. For these levels experiments on our forward and backward signal separation procedure have not been performed. Instead, we have assumed that they have the same angular distributions as for $v' = 0$. This is supported by the fact that angular distributions depend on the initial and final electronic states and not upon the individual vibrational levels, and also by comparison to the angular behavior of different vibrational levels excitation as reported by Zobel *et al.* [12]. Therefore, using DCS ratios for $v' = 0$, for considered electron energies, differential cross sections at 0° and at 180° are also estimated for the $v' = 1$–5 levels. These results are also shown in Figs. 2 and 3.

As it can be seen from Figs. 2 and 3, differential cross sections at 180° are higher than those at 0° for all vibrational
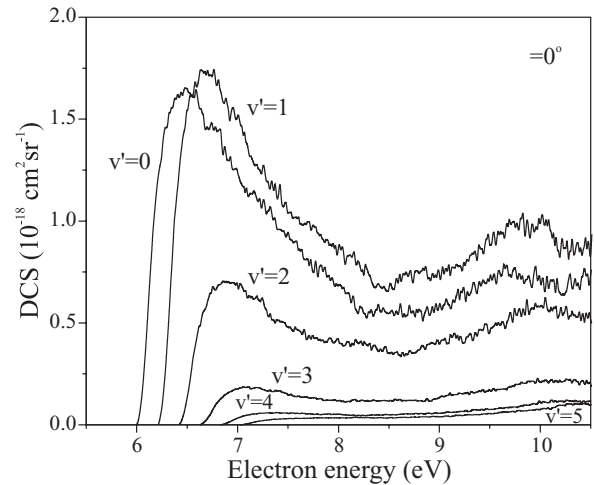
FIG. 2. Differential cross sections at 0° for excitation of $v' = 0$–5 levels of the $a\,^3\Pi$ state of CO.

levels and for all energies for a factor of about 2 up to 5. It is also interesting that the shapes of the DCSs with the energy are different in these two cases. At 0° all the levels have a pronounced maximum around the 7 eV, are falling rapidly, and then have another local maximum near 10 eV. On the other hand, at 180° all the DCSs are uniform above threshold and are decreasing just above 10 eV. This behavior can be compared, although not fully adequately, with the calculations of Morgan and Tennyson [14], with resonant excitation via three possible intermediate resonances. From the energy dependence of the integrated cross section of the considered transitions, we can draw the conclusion that at low scattering angles excitation takes place via the $^2\Pi$ and $^2\Delta$ resonances and at backward scattering angles the $^2\Pi$ and $^2\Sigma$ resonances are dominant.

The present results are also compared with other experimental and theoretical results. In Fig. 4 the angular distributions for incident electron energies of 6.5, 7, 8, 9, and 9.7 eV are presented. Our results are in very good agreement with the data of Zobel *et al.* [12], especially having in mind that the normalization procedures of these measurements were
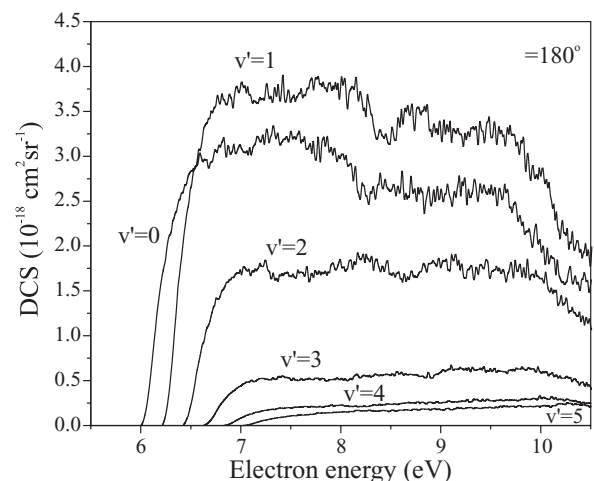
FIG. 3. Differential cross sections at 180° for excitation of $v' = 0$–5 levels of the $a\,^3\Pi$ state of CO.
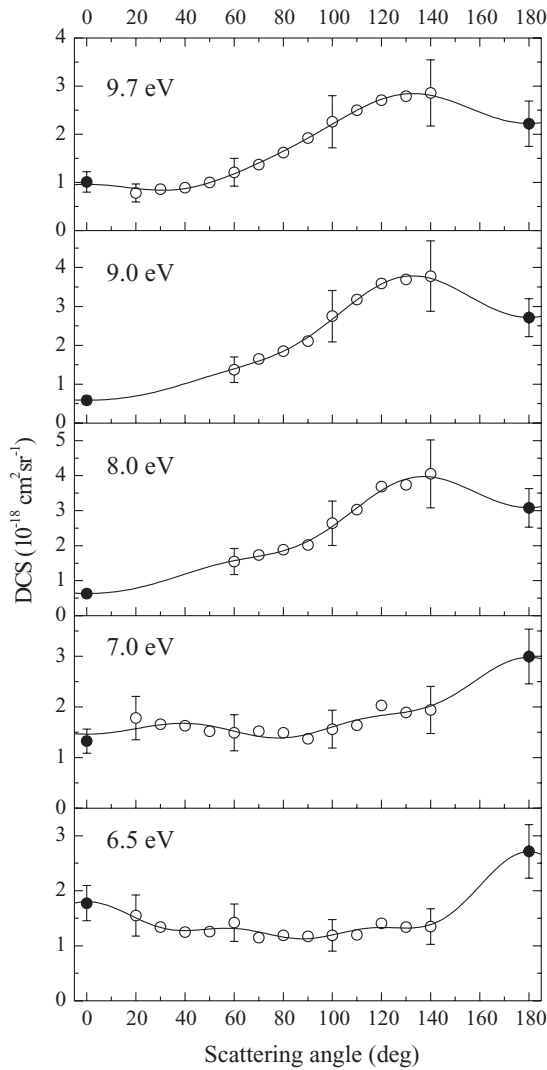
FIG. 4. Differential cross sections for the $v' = 0$ level excitation of the $a\,^3\Pi$ state of CO at indicated electron energies: present results (solid circles); Zobel *et al.* (open circles); Legendre polynomial fit (full line).

TABLE II. The Franck-Condon factors (FCF) and estimated ICS values (in 10^{-18} cm^2) for the excitation of the $v' = 0$–5 levels of $a\,^3\Pi$ for indicated electron energies.

v'	0	1	2	3	4	5
FCF	0.71	1	0.62	0.21	0.04	0.004
6.5 eV	16.62	23.41	14.50	4.90	0.95	0.10
7.0 eV	21.36	30.09	18.63	6.29	1.21	0.12
8.0 eV	30.10	42.40	26.25	8.87	1.71	0.17
9.0 eV	29.05	40.92	25.34	8.56	1.65	0.16
9.7 eV	23.61	33.26	20.59	6.96	1.34	0.13

In order to estimate the ICS for higher v' levels, we have determined the Franck-Condon factors for the transitions from the $v = 0$ of the ground $^1\Sigma^+$ state to the $v' = 0, 1, 2, 3, 4$, and 5 levels of the $a\,^3\Pi$ state. They are found to be 0.71, 1, 0.62, 0.21, 0.04, and 0.004, respectively (see Table II). The present values are in a fairly good agreement with the results of Zobel *et al.* [12] and Halman and Laulicht [31]. Our values are used, together with the ICS values for $v' = 0$ from Table I, to determine corresponding ICS values for the $v' = 1, 2, 3, 4$, and 5 levels for the considered electron energies. The results are listed in Table II. In general, the present results are in a reasonable agreement with the most recent ICS results of Zobel *et al.* [12]. This will be considered in more detail in our forthcoming paper.

In order to compare our results with the SMC variational method of Sun *et al.* [16], we summed all the particular ($v' = 0$–5) DCS contributions for excitation of the $a\,^3\Pi$ state. These data, together with the one of Zobel *et al.* [12], LeClair *et al.* [10], and Sun *et al.* [16] for the incident electron energy of 8 eV are presented in Fig. 5. A Legendre polynomial fit of all the experimental data (Zobel *et al.* [12], Le Clair *et al.* [10], and the present results) in the overall angular range is also shown in Fig. 5. The agreement between this fit and the theoretical prediction of Sun *et al.* [16] is evident, both in shape and in magnitude.

completely independent. Estimated errors associated with the present DCS values include error bars of the data used for normalization (12%), error bars due to our normalization procedure (12%), and error bars of our signal separation procedure (which is 5% for all cases and 10% for 9.7 eV). The total uncertainties are found to be 18% for all cases and 20% in the case of 9.7 eV impact energy.

It can also be seen from Fig. 4 by the comparison with the theoretical findings of Morgan and Tennyson [14] that the contribution of the $^2\Pi$ resonance to the DCS is dominant for energies above 8 eV and for higher scattering angles, but it is not negligible even for lower energies.

The fit of the experimental data by Legendre polynomials, also shown in the figures, can be used for an accurate determination of the integral cross section values. Estimated ICS values for $v' = 0$ transition for the considered electron energies are presented in Table I. Error bars for the ICS values are calculated by integrating 90% confidence bands of the polynomial fit. They are found to be 20% in all cases.

FIG. 5. Total DCS for the excitation of the $a\,^3\Pi$ state of CO at 8 eV: present results (solid circles); Zobel *et al.* (open circles); LeClair *et al.* (solid square); Sun *et al.* (dashed line); and experimental data fit (full line).

IV. CONCLUSIONS

Electron impact vibrational excitation of the $v' = 0$–5 levels of the valence $a\,^3\Pi$ state of CO has been investigated in the energy region from threshold to 9.7 eV. The ratios of DCS at $0°$ and $180°$ for the $v' = 0$ vibrational level are measured. Absolute DCS values have been determined by normalization to the ground level vibrational excitation via the $^2\Pi$ resonance. Present results have removed the long standing lack of experimental DCS data at the border angles of $0°$ and $180°$. The present results are also in good agreement with the available literature data, both experimental and theoretical. Due to the specific form of the angular distributions in the low-energy region, these results can be useful for more sophisticated modeling of CO discharges, in particular in the presence of external electric and magnetic fields. Further theoretical development in this field is also expected.

[1] J. Hahn and C. Junge, Z. Naturforsch. A **32**, 190 (1977).

[2] G. N. Pearson and D. R. Hall, J. Phys. D: Appl. Phys. **22**, 1102 (1989).

[3] L. Campbell and M. J. Brunger, PMC Phys. B **1**, 3 (2008).

[4] M. L. Sitko, L. S. Bernstein, and R. J. Glinski, Astrophys. J. **680**, 1426 (2008).

[5] G. J. Schulz, Rev. Mod. Phys. **45**, 423 (1973).

[6] S. Trajmar, D. F. Register, and A. Chutjian, Phys. Rep. **97**, 219 (1983).

[7] M. J. Brunger and S. J. Buckman, Phys. Rep. **357**, 215 (2002).

[8] S. Trajmar, W. Willians, and D. C. Cartwright, Proceedings VII ICPEAC (1971), p. 1066.

[9] A. G. Middleton, M. J. Brunger, and P. J. O. Teubner, J. Phys. B **26**, 1743 (1993).

[10] L. R. LeClair and S. Trajmar, J. Phys. B **29**, 5543 (1996).

[11] P. W. Zetner, I. Kanik, and S. Trajmar, J. Phys. B **31**, 2395 (1998).

[12] J. Zobel, U. Mayer, K. Jung, and H. Ehrhardt, J. Phys. B **29**, 813 (1996).

[13] S. K. Srivastava, A. Chutjian, and S. Trajmar, J. Chem. Phys. **63**, 2659 (1975).

[14] L. A. Morgan and J. Tennyson, J. Phys. B **26**, 2429 (1993).

[15] L. Mu-Tao and W. McKoy, J. Phys. B **15**, 3971 (1982).

[16] Q. Sun, C. Winstead, and V. McKoy, Phys. Rev. A **46**, 6987 (1992).

[17] L. Mu-Tao, A. M. Machado, M. M. Fujimoto, L. E. Machado, and L. M. Brescansin, J. Phys. B **29**, 4285 (1996).

[18] J. M. Ajello, J. Chem. Phys. **55**, 3158 (1971).

[19] H. H. Brongersma, A. J. H. Boerboom, and J. Kistemaker, Physica **44**, 449 (1969).

[20] J. E. Land, J. Appl. Phys. **49**, 5716 (1978).

[21] D. S. Newman, M. Z. M, and G. C. King, J. Phys. B: At. Mol. Phys. **16**, 2247 (1983).

[22] J. M. Furlong and W. R. Newell, J. Phys. B **29**, 331 (1996).

[23] S. Chung and C. C. Lin, Phys. Rev. A **9**, 1954 (1974).

[24] M. Vićić, G. Poparić, and D. S. Belić, Rev. Sci. Instrum. **69**, 1996 (1998).

[25] G. B. Poparić, M. D. Vićić, and D. S. Belić, Phys. Rev. A **66**, 022711 (2002).

[26] G. B. Poparić, S. M. D. Galijaš, and D. S. Belić, Phys. Rev. A **70**, 024701 (2004).

[27] M. Allan, J. Electron Spectrosc. Relat. Phenom. **48**, 219 (1989).

[28] K. R. Asmis and M. Allan, J. Phys. B **30**, 1961. (1997).

[29] G. B. Poparić, D. S. Belić, and M. M. Ristić, Phys. Rev. A **82**, 012706 (2010).

[30] G. B. Poparić, D. S. Belić, and M. D. Vićić, Phys. Rev. A **73**, 062713 (2006).

[31] M. Halman and I. Laulicht, Astron. Phys. J. (Suppl.) **12**, 307 (1965).